Available online at www.sciencedirect.com
ScienceDirect
Trans. Nonferrous Met. Soc. China 30(2020) 1500−1510
Transactions of Nonferrous Metals Society of China
www.tnmsc.cn

Evolution of precipitates in Mg−7Gd−3Y−1Nd−1Zn−0.5Zr alloy with fine plate-like 14H-LPSO structures aged at 240 °C

Yong-gang PENG[1,2,3,4], Zhi-wei DU[1,2,3,4], Wei LIU[5], Yong-jun LI[6], Ting LI[1,2,3,4], Xiao-lei HAN[1,2], Ming-long MA[6], Zheng PANG[1,2,3,4], Jia-wei YUAN[6], Guo-liang SHI[6]

1. National Center of Analysis and Testing for Nonferrous Metals and Electronic Materials, GRINM Group Co., Ltd., Beijing 100088, China;
2. Guobiao (Beijing) Testing & Certification Co., Ltd., Beijing 100088, China;
3. Beijing General Research Institute for Non-ferrous Metals, Beijing 100088, China;
4. China United Test & Certification Co., Ltd., Beijing 100088, China;
5. Beijing Chunlizhengda Medical Instruments Co., Ltd., Beijing 101100, China;
6. State Key Laboratory of Non-ferrous Metals & Processes, GRIMAT Engineering Institute Co., Ltd., Beijing 101407, China

Received 22 October 2019; accepted 14 April 2020

Abstract: The morphology and crystal structure of the precipitates in Mg−7Gd−3Y−1Nd−1Zn−0.5Zr (wt.%) alloy with fine plate-like 14H-LPSO structures aged at 240 °C were investigated using transmission electron microscopy (TEM) and high-angle annular dark-field scanning transmission electron microscopy (HAADF-STEM). Fine plate-like 14H-LPSO structures precipitate after heat treatment at 500 °C for 2 h, and β-type phases precipitate after the alloy is aged at 240 °C. The long-period atomic stacking sequence of 14H-LPSO structures along the $[0001]_\alpha$ direction is ABABCACACACBABA. After being aged at 240 °C for 2 h, the β-type phases are the ordered solution clusters, zig-zag GP zones, and a small number of β' phases. The peak hardness is obtained at 240 °C for 18 h with a Brinell hardness of 112, the β-type phases are β' phases and local RE-rich structures. After being aged at 240 °C for 100 h, the β-type phases are β', β_1 and β'_F phases. β' phases nucleate from the zig-zag GP zones directly without β'' phases, and then transform into β_1 phase by $\beta'\rightarrow\beta'_F\rightarrow\beta_1$ transformations. The Zn not only can form LPSO structure, but also is the constituent element of β_1 phases. LPSO structures have a certain hindrance to the coarsening of β' and β_1 along $\langle 0001\rangle_\alpha$.
Key words: magnesium alloy; ageing; precipitates; long-period stacking ordered (LPSO) structures; HAADF-STEM

1 Introduction

Magnesium and its alloys, the lightest structural material, have attracted increasing attention in aerospace, automotive, aircraft and 3C (computer, communication and consumer electronic product) industries and so on [1−3]. However, the poor mechanical properties and corrosion resistance limit widespread applications of magnesium alloys. It has been reported that Mg−Gd−Y-based alloys exhibits ultra-high strength [4−6]. Addition of Zn into Mg−Gd−Y-based alloys can form LPSO structure, which usually exhibit high strength, high ductility and high creep-resistance [7−10].

Many magnesium alloys can achieve their excellent mechanical properties via age hardening. The precipitation sequence of Mg−Gd(−Y) during

Foundation item: Projects (51871195, 51501015) supported by the National Natural Science Foundation of China; Project (TC170A5SU-1) supported by Ministry of Industry and Information Technology of China
Corresponding author: Zhi-wei DU, Tel: +86-10-82241349, E-mail: duzhiwei@gbtcgroup.com;
Yong-jun LI, Tel: +86-13601076520, E-mail: liyongjun8158@163.com
DOI: 10.1016/S1003-6326(20)65314-6

isothermal ageing has been proposed as follows: α-Mg super-saturated solid solution (S.S.S.S) → ordered G.P. zones → β'' (Mg_3Gd) → β' (Mg_7Gd)→ β_1 (Mg_3Gd) → β (Mg_5Gd) [11]. However, ZHENG et al [12] considered that the existence of reported β'' structure is doubted in Mg−Gd−Y alloy. ZHANG et al [13] reported a detailed precipitate evolution in Mg−Gd alloy without β'': super-saturated solid solution (S.S.S.S.) → ordered solute clusters → GP zones → β' → β'_F + tail-like hybrid structures → β_1 → β. The precipitate at peak ageing stage was β' phase [14,15].

LPSO structure can strengthen the alloys without sacrificing the ductility [16]. LPSO structure can exhibit different polytypes, 10H [17], 14H [18], 18R [18] and 24R [19], among which 14H and 18R structures have been most frequently observed in Mg−Gd−Y−Zn alloys [6−8]. Probable transformation sequence of LPSO precipitate plates in the α-Mg matrix is: single building block → various metastable LPSO building block clusters → 14H, and the probable transformation sequence in the interdendritic LPSO structure is: 18R → various metastable LPSO building block clusters → 14H [20].

The age hardening effect is depended on the size, number density, morphology, orientation and structure of precipitates. The strengthening effect of LPSO structure depends sensitively on size and morphology [9,10]. LI et al [21,22] proposed a potentially effective approach, benefiting LPSO and β' phase, to develop new Mg−RE based alloys with high strength, high ductility and high creep-resistance. So far, only a few studies have addressed the relationship between the LPSO and the β-type precipitates. ZHENG and CHEN [23] reported an atomic-scale investigation into the spatial relations and interactions between β' phases and long-period stacking ordered (LPSO) structure in Mg−10Gd−5Y−2Zn−0.5Zr (wt.%) alloy. Therefore, there remains a need for a systematic examination of the relation of the LPSO and the β-type precipitates. Besides, Zn added into Mg−Gd−Y-based alloys can form LPSO structure, but the effect of Zn on β-type precipitates is not clearly revealed.

In previous study, the ageing-hardening curve of Mg−7Gd−5Y−1Nd−0.5Zr alloy has a long period of peak plateau with high Brinell hardness during 18−180 h, and the precipitate in peak ageing stage was β' phase [15]. The elongation of the as-extruded Mg−7Gd−3Y−1Nd−1Zn−0.5Zr alloy with the fine plate-like 14H-LPSO structures was higher than that of the alloy without the fine plate-like 14H-LPSO structures [24]. LIU et al [25] proposed the schematic diagram of relationship among the LPSO, β' and β_1. This work provides an atomic-scale structural analysis of the evolution of LPSO and β-type phases. The effect of LPSO structure on β-type phases aged at 240 °C of Mg−7Gd−3Y−1Nd−1Zn−0.5Zr alloy (wt.%) using transmission electron microscopy (TEM) and high resolution high-angle annular dark-field scanning transmission electron microscopy (HAADF-STEM) is investigated.

2 Experimental

The Mg−7Gd−3Y−1Nd−1Zn−0.5Zr (wt.%) alloy was melted in an electrical resistance furnace. The ingot was cut into 10 mm × 10 mm × 10 mm small bulks that were homogenized at 525 °C for 48 h, and quenched into warm water at 30 °C. The eutectic phase and LPSO structure formed during the casting process and were dissolved into the matrix during the solution-treatment at 525 °C for 48 h. Subsequently, the homogenized samples were heated at 500 °C for 2 h to precipitate LPSO structures, and then followed by ageing at 240 °C. The hardness of the samples was measured by Brinell hardness tester with a loading force of 612.5 N and dwelling time of 25 s. Thin foils (3 mm in diameter) for TEM were prepared by mechanical polishing (~50 μm) and then twin-jet electro-polished in a solution of 3 vol.% perchloric acid and 97 vol.% ethanol, at temperature from −30 to −40 °C and the current of 15 mA. Finally, the foils were cleaned by the Gatan Precision Ion Polishing System (PIPS, GATAN 695) at −120 °C for 30 min under low incidental angle and low voltage. The bright field (BF), high-resolution transmission electron microscopy (HRTEM) and the high-angle annular dark-field scanning transmission electron microscopy (HAADF-STEM) images of the precipitates in the over ageing stage were analyzed by Tecnai G2 F20−TWIN transmission electron microscope equipped with an energy-dispersive X-ray spectrometer (EDS), operating at 200 kV. The atomic-scale HAADF-STEM images of the β-type phases in aging stage and over ageing stage were analyzed by

JEM-ARM200F atomic resolution analytical microscope equipped with a STEM Cs corrector operating at 200 kV. The EDS elemental maps were analyzed by JEOL Dual SDD attached to the JEM-ARM200F.

3 Results and discussion

3.1 Heat treatment at 500 °C for 2 h

Figure 1(a) shows the bright filed (BF) TEM image of the alloy and corresponding selected area electron diffraction (SAED) pattern taken along the $[0001]_\alpha$, after heat treatment at 500 °C for 2h. As shown in Fig. 1(a), there are no obvious diffraction spots in the SAED pattern, and no any other precipitate was observed from the BF image, which indicates that no β-type phases precipitate. Figure 1(b) shows HAADF-STEM image and corresponding SAED pattern taken along the $[11\bar{2}0]_\alpha$. Viewed from $[11\bar{2}0]_\alpha$, there are many nanoscale fine plate-like LPSO structures precipitating along the base surface $(0001)_\alpha$ as marked by white arrows. Corresponding SAED pattern (insert in Fig. 1(b)) indicates that the fine plate-like precipitates are of 14H-LPSO structures, where thirteen extra diffraction spots are observed between $(0000)_\alpha$ and $(0002)_\alpha$.

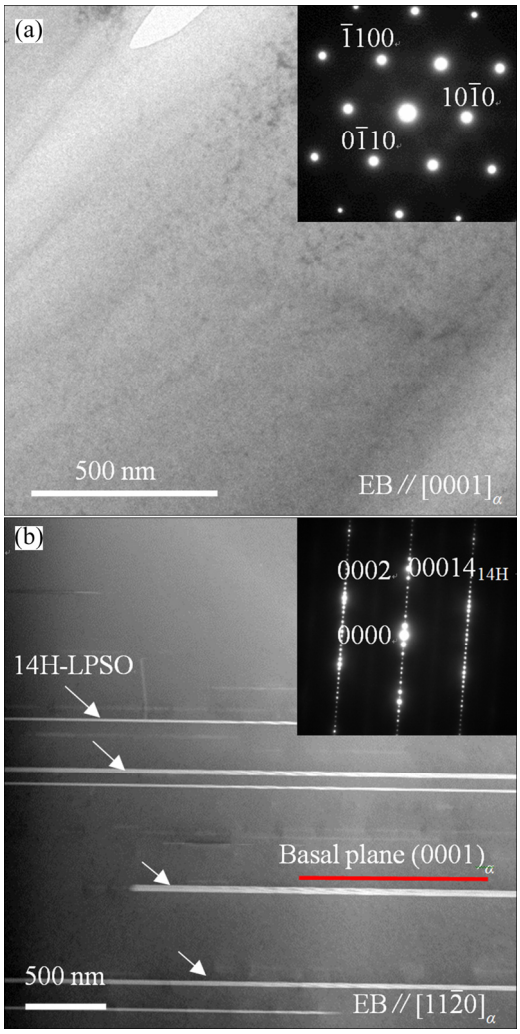

Fig. 1 Microstructures of Mg−7Gd−3Y−1Nd−1Zn−0.5Zr alloy after heat treatment at 500 °C for 2 h: (a) Bright filed (BF) image and corresponding SAED pattern from $[0001]_\alpha$; (b) HAADF-STEM image and corresponding SAED pattern from $[11\bar{2}0]_\alpha$

3.2 Hardness response

The Brinell hardness value of as-homogenized alloy is 78, and the Brinell hardness value of the alloy after heat treatment at 500 °C for 2 h is 86. A large number of 14H-LPSO structures lead to increased hardness after heat treatment at 500 °C for 2 h. This is because 14H-LPSO structures are harder than α-Mg matrix owing to higher contents of Gd and Zn elements. Mg−7Gd−3Y−1Nd−1Zn−0.5Zr (wt.%) alloy shows a typical hardness response while ageing at 240 °C, as presented in Fig. 2. Initially, the hardness increases slowly, and increases rapidly after 240 °C for 2 h. And the peak hardness is obtained at 240 °C for 18 h with a peak hardness of 112, which is higher than that the sample (106) aged at 240 °C directly [25]. Besides, there is a long period of plateau during 30−200 h in the over-ageing stage, rather than in the peak-ageing stage. And the Brinell hardness of the plateau is lower than that of the sample aged at 240 °C directly, which can be attributed to the formation of LPSO structure that consumes RE (Zn), and reduces the content of RE (Zn) in Mg

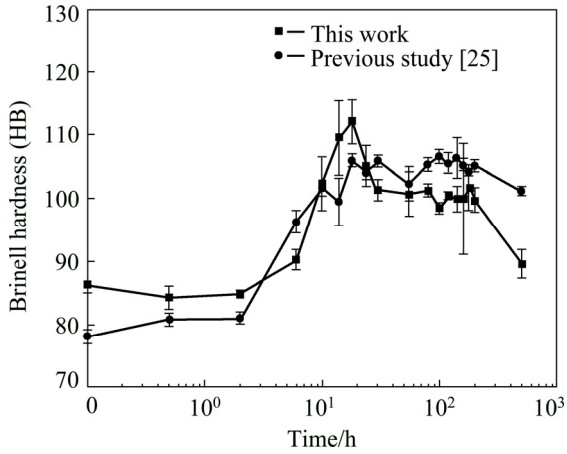

Fig. 2 Ageing-hardening curves of Mg−7Gd−3Y−1Nd−1Zn−0.5Zr alloy aged at 240 °C

matrix. The long period of plateau suggests that the main strengthening phases precipitating in the alloy have good thermal stability. In order to further understand the precipitation behavior of the alloy with fine plate-like LPSO structures in ageing stage, the microstructures of the alloy were analyzed in this study.

3.3 Ageing at 240 °C for 2 h

Figure 3 shows the atomic resolution HAADF-STEM image of ordered solute clusters and zig-zag GP zones (Fig. 3(a)), and low-magnification HAADF-STEM image of β' phases (Fig. 3(b)) from $[0001]_\alpha$ aged at 240 °C for 2 h. Since the brightness of individual atomic columns in HAADF-STEM images approximates proportionally to the square of the averaged atomic number, each bright dot represents a column rich in RE (Zn) atoms [26,27]. Figure 3(a) shows the existence of a large number of ordered solution clusters (marked by yellow arrows and yellow dotted circles) of different compact forms and zigzag Guiniere Preston (GP) zones (marked by red dotted circles). In addition to the single hexagonal ring structure (marked by yellow dotted circles) containing six bright contrast dots, many short-range ordering structure (marked by yellow arrows) containing 1−5 RE (Zn) atom columns are observed. All the short-range ordered structures containing 1−6 RE-rich atom columns can be classified as ordered solute clusters [26]. Meanwhile, a small amount of zig-zag arrays with the habit planes parallel to $\{1\bar{1}00\}_\alpha$ are observed (marked by red dotted circles). These zig-zag arrays are considered to be prismatic GP zones [26]. The zig-zag arrays are consistent with β' structure, and the single zig-zag array is a repetitive unit in β' structure. β' phases (marked by red arrows) are observed in Fig. 3(b), so it is assumed that β' can nucleate from the zig-zag arrays directly without β'' phase. The ordered solution clusters, zig-zag GP zones, and a small number of β' phases have little strengthening effect, so the Brinell hardness doesn't increase after the alloy is aged at 240 °C for 2 h in Fig. 2.

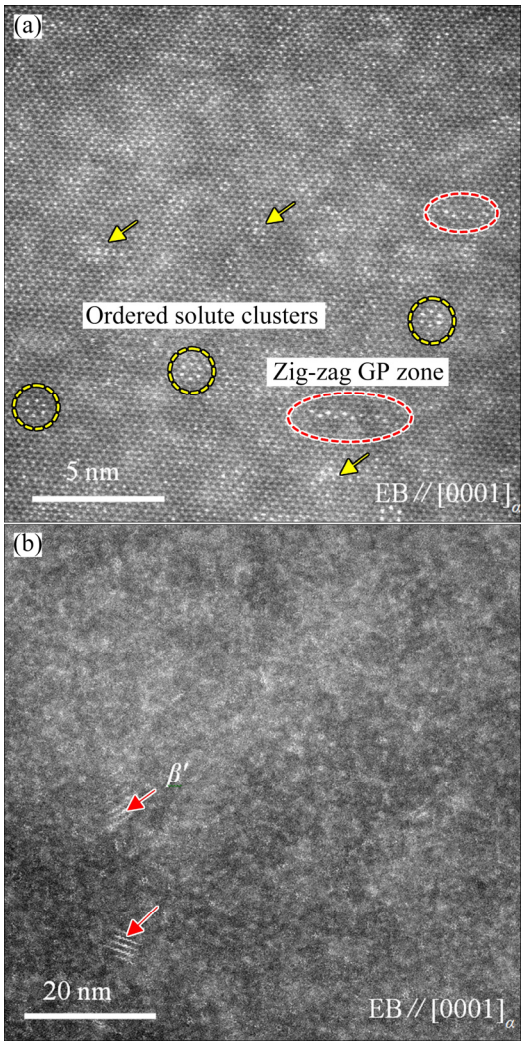

Fig. 3 Microstructures of Mg−7Gd−3Y−1Nd−1Zn−0.5Zr alloy aged at 240 °C for 2 h with electron beam parallel to $[0001]_\alpha$: (a) Atomic resolution HAADF-STEM image showing ordered solute clusters and zig-zag GP zones; (b) HAADF-STEM image of β' phases

Figure 4 shows the HAADF-STEM images, SAED pattern and HRTEM image of Mg−7Gd−3Y−1Nd−1Zn−0.5Zr (wt.%) alloy aged at 240 °C for 2 h along the $[11\bar{2}0]_\alpha$. There are many nanoscale fine plate-like 14H-LPSO structures, with corresponding SAED pattern shown in Fig. 4(b). Figure 4(c) shows the enlarged HAADF-STEM image of Fig. 4(a). It can be seen that LPSO structure consists of diverse numbers of building blocks of four close-packed layers with bright contrast, and the building blocks are separated by diverse numbers of α-Mg layers in different types of metastable LPSO structure [20]. The bright contrast of the building block is due to the enrichment of RE (Zn) atoms. EDS analysis results show that the composition of the 14H-LPSO structure (Point A in Fig. 4(b)) is 87.90Mg−3.58Gd−2.67Y−0.57Nd−5.28Zn (at.%), and the composition of the α-Mg matrix (Point B in Fig. 4(b)) is 97.67Mg−1.36Gd−0.72Y−0.25Nd (at.%). Compared to α-Mg matrix, the contents of Gd, Y, Nd and Zn are higher in 14H-LPSO

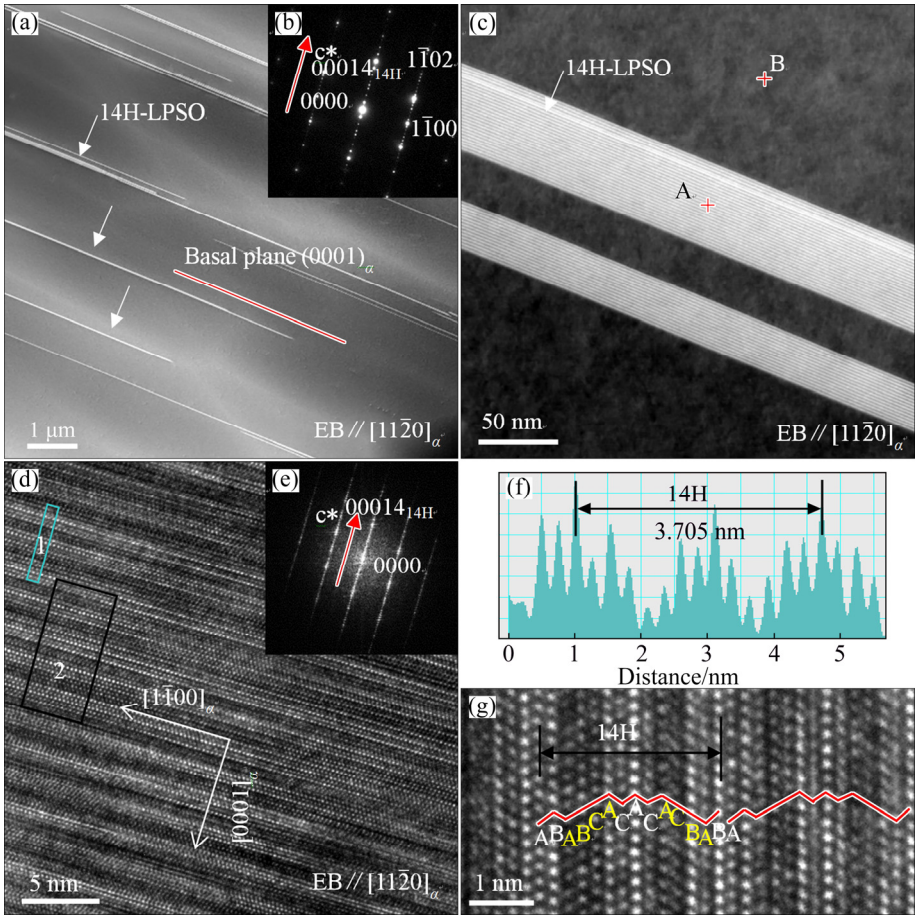

Fig. 4 Microstructures of Mg−7Gd−3Y−1Nd−1Zn−0.5Zr alloy aged at 240 °C for 2 h with electron beam parallel to $[11\bar{2}0]_\alpha$: (a) Low-magnification HAADF-STEM image; (b) Corresponding SAED pattern of Fig. 4(a); (c) Enlarged HAADF-STEM image of Fig. 4(a); (d) HRTEM image; (e) Corresponding Fast Fourier Transform (FFT) pattern of Fig. 4(d); (f) Profile of Zone 1 in Fig. 4(d); (g) Enlarged HRTEM image of Zone 2 in Fig. 4(d)

structure, especially Zn content. The composition of the LPSO structure is confirmed to be Mg_{12}(Gd,Y,Nd)Zn, or Mg_{12}REZn. Figure 4(d) shows a low-magnification HRTEM image of the LPSO structure, and the corresponding Fast Fourier Transform (FFT) pattern is shown in Fig. 4(e). Figure 4(f) shows the profile of Zone 1 in Fig. 4(d). The 14H unit cell contains 14 layers of closely packed planes, with a height of 3.705 nm along the packing direction, as shown in Figs. 4(f, g). An enlarged HRTEM image of Zone 2 is shown in Fig. 4(g). A long-period atomic stacking sequence along the $[0001]_\alpha$ direction is ABABCACACACBABA, with "ABCA" and "ACBA" in the opposite direction, which is consistent with that of 14H in Mg−Y−Zn alloy [18].

3.4 Ageing at 240 °C for 18 h

Figure 5 shows the HAADF-STEM image, SAED pattern and HRTEM image of Mg−7Gd−3Y−1Nd−1Zn−0.5Zr (wt.%) alloy aged at 240 °C for 18 h, taken with the incident electron beam parallel to $[0001]_\alpha$ and $[11\bar{2}0]_\alpha$, respectively. As shown in Fig. 5(a), bamboo-like fine precipitates uniformly disperse within the alloy with three variants (marked by red arrows), and the mid-rib planes of three variants are parallel to $(11\bar{2}0)_\alpha$, $(1\bar{2}10)_\alpha$, and $(\bar{2}110)_\alpha$, respectively. These three variants of the precipitates are related to each other by 120° rotation around $[0001]_\alpha$. The length of precipitates is 5−15 nm along $\langle 11\bar{2}0\rangle_\alpha$, and 6−21 nm along $\langle 10\bar{1}0\rangle_\alpha$, and the length-to-width ratio is 0.8−2.8. Corresponding SAED pattern shown in Fig. 5(b) can be indexed consistently according to the base-centered orthorhombic (b.c.o.) structure with lattice parameters of a=0.64 nm, b=2.22 nm and c=0.52 nm, which indicates that the fine precipitates are β' phases [15]. The orientation relationship between β' phase and α-Mg is $(100)_{\beta'}$ // $(11\bar{2}0)_\alpha$, $[0001]_\alpha$ // $[001]_{\beta'}$, and the habit

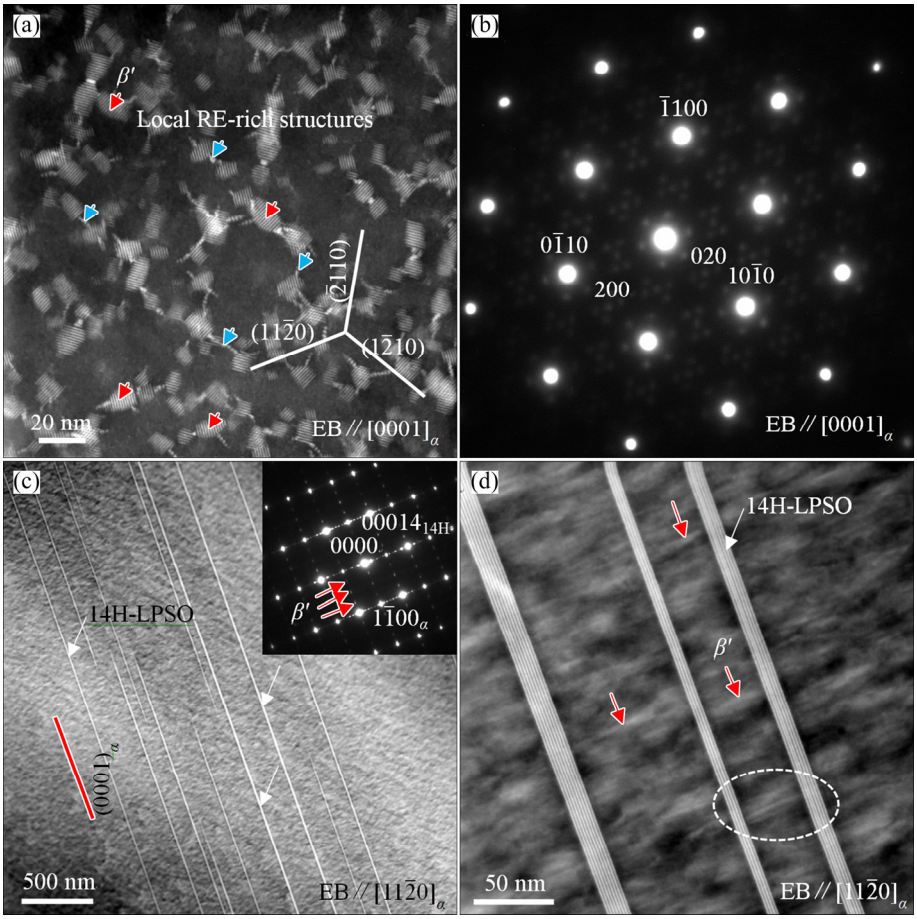

Fig. 5 Microstructures of Mg−7Gd−3Y−1Nd−1Zn−0.5Zr alloy aged at 240 °C for 18 h: (a) HAADF-STEM image from $[0001]_\alpha$; (b) Corresponding SAED pattern of Fig. 5(a); (c) Low-magnification HAADF-STEM image and corresponding SAED pattern from $[11\bar{2}0]_\alpha$; (d) Enlarged HAADF-STEM image from $[11\bar{2}0]_\alpha$

plane is parallel to $\{11\bar{2}0\}_\alpha$. Meanwhile, tail-like structure protrusions (marked by blue arrows) located at the ends of the β' phases are observed, which are also reported in Mg−Gd−Zn [28], Mg−Gd−Ag−Zr [29] alloys. Tail-like structure protrusions are local RE-rich structures, consisting of multiple hexagonal ring structures, and nucleate from ordered solute clusters.

Figures 5(c, d) show the HAADF-STEM images of the LPSO structure, and corresponding FFT pattern is shown in the inset of Fig. 5(c), with the incident electron beam parallel to $[11\bar{2}0]_\alpha$. In addition to 14H-LPSO structure, there are obvious diffracted spots of β' phases in the corresponding SAED pattern in Fig. 5(d). The β' phase (marked by red arrows) is still bamboo-like in the $[11\bar{2}0]_\alpha$ direction, and the length of β' phases is 20−50 nm along $\langle 0001\rangle_\alpha$. At the same time, none of β' passes through the LPSO structure, as shown in the white dotted circle in Fig. 5(d), so LPSO structure has a certain hindrance to the coarsening of β'.

The alloy reaches its peak hardness when ageing at 240 °C for 18 h. LPSO structure, largely dispersed β' phases and local RE-rich structures take the major role in hardening the alloy. In the under-ageing stage, the increase in Brinell hardness in Fig. 2 is caused by the nucleation and growth of β' phases and local RE-rich structures. The reason why the peak hardness is obtained at 18 h, while peak-ageing plateau appears without an obvious peak ageing at 240 °C directly (Fig. 2), remains unclear.

3.5 Ageing at 240 °C for 100 h

Figure 6 shows the BF and HAADF-STEM images of the alloy aged at 240 °C for 100 h, and the incident electron beam is parallel to $[0001]_\alpha$. After 100 h ageing, the majority of the precipitates are β' (marked by red arrows) and β_1 (marked by yellow arrows) phases, as shown in Figs. 6(a, b). The overlapped diffraction pattern inserted in Fig. 6(a) shows that the orientation relationship

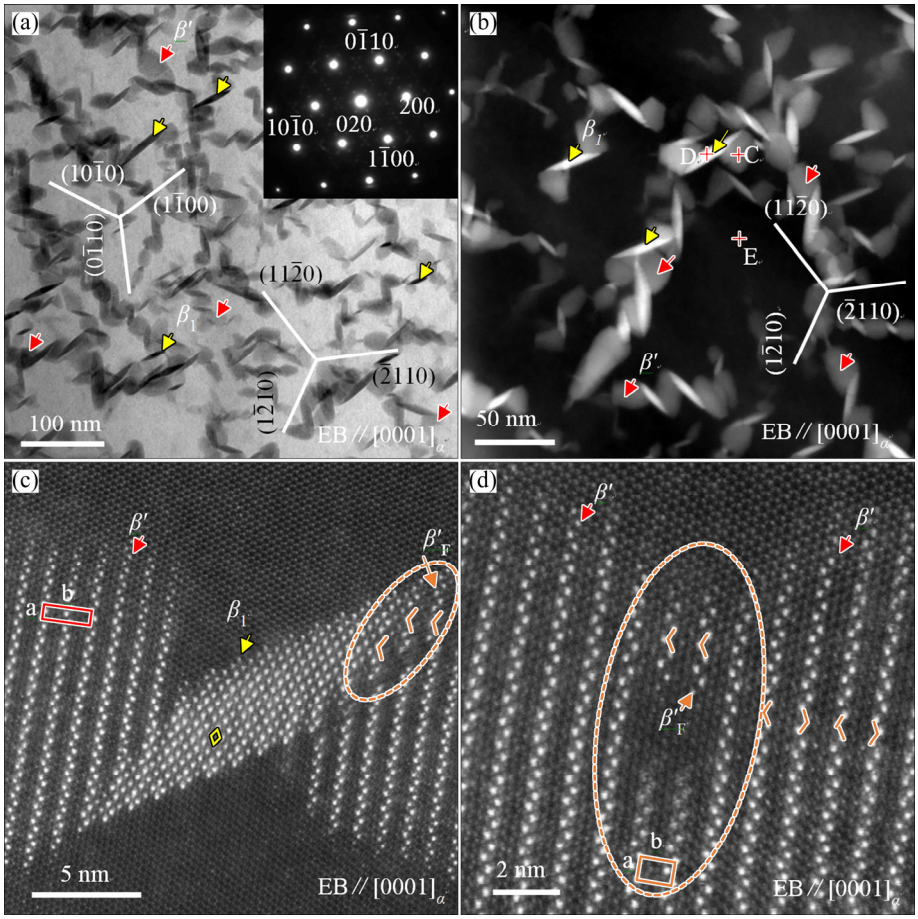

Fig. 6 Microstructures of Mg−7Gd−3Y−1Nd−1Zn−0.5Zr alloy aged at 240 °C for 100 h from $[0001]_\alpha$: (a) BF image and corresponding SAED pattern; (b) Low-magnification HAADF-STEM image; (c, d) Atomic resolution HAADF-STEM images of β', β_1 and β'_F phases

between the β' phases and the matrix does not change during ageing. A single β' phase has a bamboo-like shape approximately 10−26 nm wide along the $\langle 11\bar{2}0\rangle_\alpha$ direction and approximately 12−36 nm long along the $\langle 10\bar{1}0\rangle_\alpha$ direction, which is larger than that of the alloy aged at 240 °C for 18 h. As shown in Fig. 6(b), β_1 phase with clearly higher contrast than the β' precipitate is observed, indicating that β_1 has a higher RE (Zn) content than β'. A single β_1 precipitate has a parallelogram shape with approximately 10−55 nm along the longer diagonal line and approximately 5−20 nm along the shorter diagonal line.

To identify the structure of β' and β_1, atomic resolution HAADF-STEM images from $[0001]_\alpha$ are shown in Figs. 6(c, d). The images show many bright dots inside the precipitates. Each bright dot represents a column rich in RE (Zn) atoms. These RE (Zn)-rich atomic columns constitute the array of zig-zag in the opposite directions in β' phases. Based on the analysis result of atomic resolution HAADF-STEM image (Fig. 6(c)), the red rectangle shows a unit cell of β' with actual lattice parameters of a=0.68 nm and b=2.26 nm. The fundamental unit of the plate-like β_1 phase (marked by yellow diamond in Fig. 6(c) has a diamond shape, composed of bright dots at its four corners. At the same time, the apexes of zig-zag arrays (marked by orange broken line) in the small particle between coarsened β' and β_1 phases (shown in Fig. 6(c)) between two coarsened β' phases (shown in Fig. 5(d)) are in the same direction, indicating that the small particle is the β'_F phase, as reported in Mg−Gd [30] and Mg−Gd−Ag−Zr [29] alloys. The β'_F phase has an orthorhombic structure, with lattice constants of a=0.64 nm, b=1.14 nm and c=0.52 nm [31]. The orange rectangle in Fig. 6(d) shows unit cell of β'_F with actual lattice parameters of a=0.72 nm and b=1.07 nm. The distance between two adjacent zig-zag arrays is about 1.1 nm, which is completely coherent with the matrix, as shown by the orange dotted circle. As shown in Fig. 6(d), β'_F

phase distributes between two β' phases, which suggests that the β'_F phase forms due to the coarsening of the β' phase. Some weak dots can be observed at the interface between the β'_F and β_1 phases (as shown in the orange dotted circle in Fig. 6(c), indicating that the β'_F phase provides a preferential nucleation site for β_1.

To distinguish the chemical nature of β' and β_1 phases, EDS elemental maps of Mg−7Gd−3Y−1Nd−1Zn−0.5Zr (wt.%) alloy aged at 240 °C for 100 h are shown in Fig. 7. The results indicate that the Gd, Y and Nd elements are obviously enriched in β' and β_1, and Zn element is obviously enriched in β_1 phase. Compared with β' phase, β_1 phase has a higher concentration of Gd, Nd and Zn. The fact that Zn element is enriched in β_1 phase was also reported in Mg−Gd−Y−Zn alloys [32]. And HONMA et al [32] think that Zn addition will enhance the precipitation of the β_1 phases, and Zn additions assist in the formation of β_1 phase [32]. β_1 phase was observed in Zn-free Mg−RE alloys [11−13], so Zn is not a required constituent element for β_1 phase.

EDS analysis results show that the composition of the β' phase (Point C in Fig. 6(b)) is 87.78Mg−7.14Gd−3.02Y−1.4Nd−0.63Zn (at.%), the composition of the β_1 phase (Point D in Fig. 6(b)) is 77.92Mg−10.87Gd−3.36Y−3.49Nd−4.36Zn (at.%), and the composition of the α-Mg matrix (Point E in Fig. 6(b)) is 99.07Mg−0.57Gd−0.34Y (at.%). β' phase is mainly composed of Mg, Gd, Y and Nd elements, and has a small amount of Zn, so the composition of β' phase is conformed to be Mg_7RE. β_1 phase mainly consists of Mg, Gd, Y, Nd and Zn elements, and compared to the β' phase, the contents of Gd, Y, Nd and Zn are increased. The composition of β_1 phase is roughly in accordance with $Mg_3(RE,Zn)$. The Mg matrix is composed entirely of Mg elements and contains a small amount of Gd and Y elements.

Figure 8 shows the HAADF-STEM images and SAED pattern of Mg−7Gd−3Y−1Nd−1Zn−0.5Zr (wt.%) alloy aged at 240 °C for 100 h along the $[11\bar{2}0]_\alpha$. The microstructure of the alloy contains β' (marked by red arrows), β_1 (marked by yellow arrows), and 14H-LPSO (marked by white arrows). Many metastable LPSO building block clusters (marked by black arrows) are observed in Fig. 8(a), and these metastable LPSO building block clusters form during ageing at 240 °C, which will transform into 14H-LPSO structures [20]. β' is still bamboo-like, and β_1 is elongated. The lengths

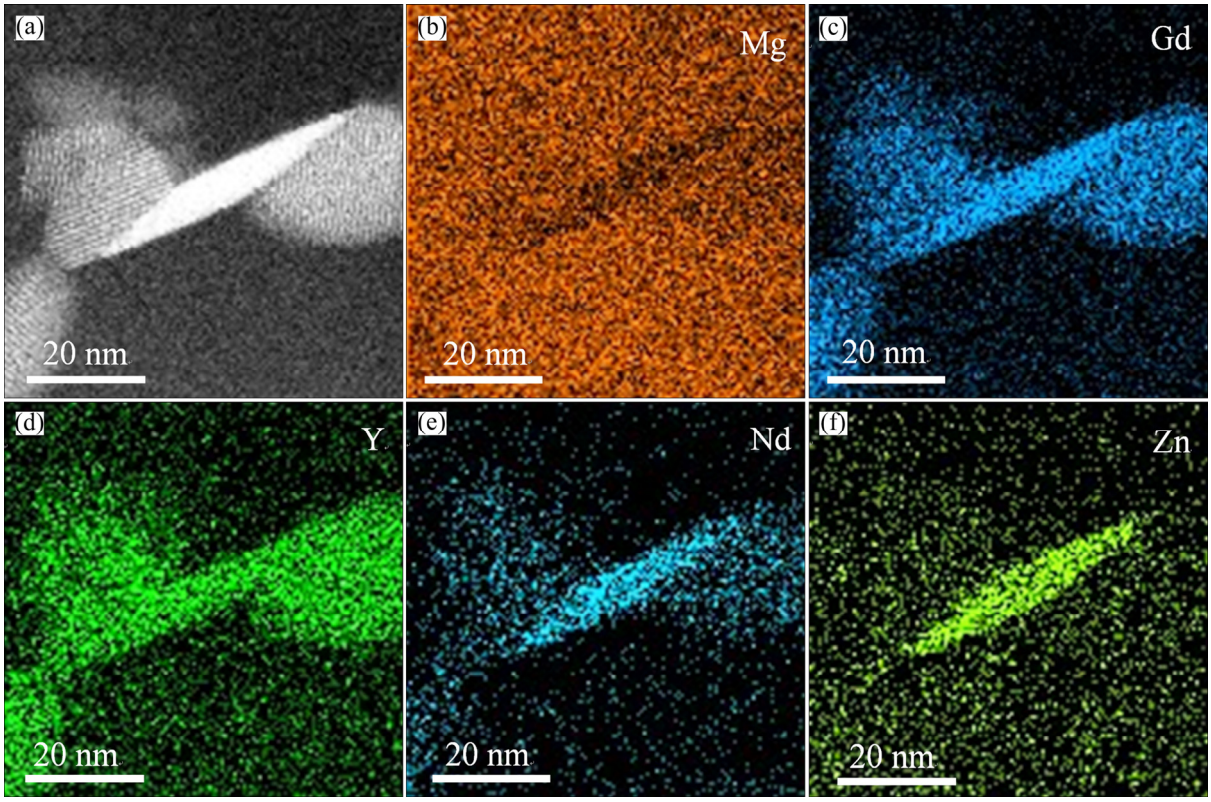

Fig. 7 EDS elemental maps of Mg−7Gd−3Y−1Nd−1Zn−0.5Zr alloy aged at 240 °C for 100 h

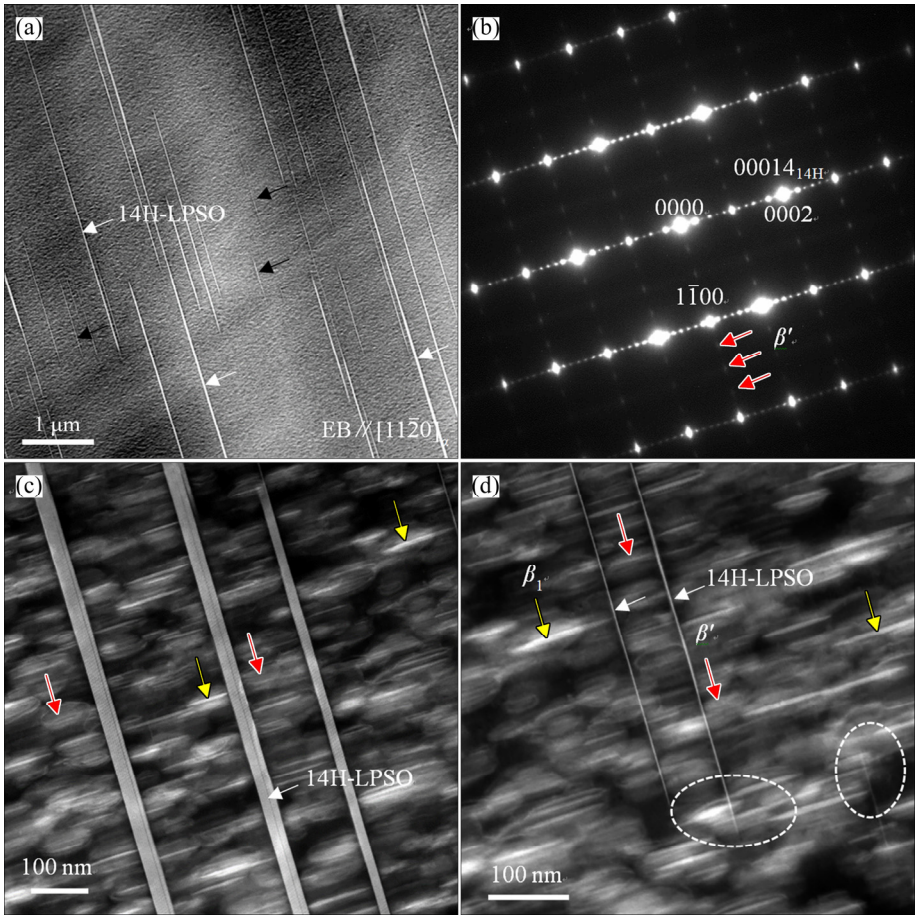

Fig. 8 Microstructures of Mg−7Gd−3Y−1Nd−1Zn−0.5Zr alloy aged at 240 °C for 100 h from $[11\bar{2}0]_\alpha$: (a) Low-magnification HAADF-STEM image of 14H-LPSO structures; (b) Corresponding SAED pattern of Fig. 8(a); (c, d) HAADF-STEM images of 14H-LPSO structures and β' and β_1 phases

of β' and β_1 in the $[0001]_\alpha$ direction are 40−130 nm and 20−120 nm, respectively. β' and β_1 phases uniformly distribute in the matrix, while the LPSO structures distribute along the base $(0001)_\alpha$. As shown in Figs. 8(c, d), both β' and β_1 do not pass through the LPSO structures, and the LPSO structure has a certain hindrance to the coarsening of β' and β_1. Some β' and β_1 phases pass the LPSO structure at the end of LPSO viewed from $[11\bar{2}0]_\alpha$, as shown in the white dotted circle in Fig. 8(d), of which the reason may be that they are at different heights along $[11\bar{2}0]_\alpha$.

After ageing at 240 °C for 100 h, the precipitates are β', β_1, β'_F and metastable LPSO building block clusters. The Brinell hardness of this stage is lower than that of the sample aged at 240 °C for 100 h directly (Fig. 1), which can be attributed to the fact that the formation of LPSO structure consumes RE (Zn), reducing the content of RE (Zn) in Mg matrix and resulting in a decrease in β-type phases such as β' and β_1. The alloy has a long period of plateau during 30−200 h in the over-ageing stage. Mg−7Gd−5Y−1Nd−0.5Zr [15] and Mg−7Gd−3Y−1Nd−1Zn−0.5Zr [25] alloys also have a long period of peak plateau. The long period of plateau suggests that the main strengthening phases precipitated in the alloy have good thermal stability [15,25].

4 Conclusions

(1) Fine plate-like 14H-LPSO structures formed after 500 °C for 2 h become coarsened and some metastable LPSO building block clusters precipitate when being aged at 240 °C. The long-period atomic stacking sequence of 14H-LPSO structures along the $[0001]_\alpha$ direction is ABABCACACACBABA.

(2) β-type phase precipitates when the alloy is aged at 240 °C. After ageing at 240 °C for 2 h, the precipitates are the ordered solution clusters, zig-zag GP zones, and a small number of β' phases,

which have little strengthening effect. After peak ageing at 240 °C for 18 h, the precipitates are β' phases and local RE-rich structures, which take the major role in hardening the alloy. After ageing at 240 °C for 100 h, the precipitates are β', β_1 and β'_F phases.

(3) The ordered solution clusters and zig-zag GP zones form directly from super saturated solid solution, and they will transform into β' phases and local RE-rich structures, respectively. The formation of the β'_F phases is supposed to be the result of the coarsening of the β' phases. β'_F phases provides a preferential nucleation site for β_1 phases.

(4) The Zn can not only form LPSO structures, but also is the constituent element of β_1 phase. The compositions of the 14H-LPSO structures, β' and β_1 phases are conformed to be $Mg_{12}REZn$, Mg_7RE and $Mg_3(RE,Zn)$, respectively. LPSO structures have a certain hindrance to the coarsening of β' and β_1 along $\langle 0001 \rangle_\alpha$.

References

[1] MORDIKE B L, EBERT T. Magnesium: Properties−application−potential [J]. Materials Science and Engineering A, 2001, 302: 37−45.

[2] AGNEW S R, NIE J F. Preface to the viewpoint set on: The current state of magnesium alloy science and technology [J]. Scripta Materialia, 2010, 63: 671−673.

[3] ZHANG J H, LIU S J, WU R Z, HOU L G, ZHANG M L. Recent developments in high-strength Mg-RE-based alloys: Focusing on Mg−Gd and Mg−Y systems [J]. Journal of Magnesium and Alloys, 2018, 6(3): 277−291.

[4] LI Y J, ZHANG K, LI X G, MA M L, WANG H Z, HE L Q. Influence of extrusion on microstructures and mechanical properties of Mg−5.0Y−7.0Gd−1.3Nd−0.5Zr magnesium alloy [J]. The Chinese Journal of Nonferrous Metals, 2010, 20(9): 1692−1697. (in Chinese)

[5] NODOOSHAN H R J, WU G, LIU W, WEI G, LI Y, ZHANG S. Effect of Gd content on high temperature mechanical properties of Mg−Gd−Y−Zr alloy [J]. Materials Science and Engineering A, 2016, 651: 840−847.

[6] YU Z J, XU C, MENG J, LIU K, FU J L, KAMADO S. Effects of extrusion ratio and temperature on the mechanical properties and microstructure of as-extruded Mg−Gd−Y−(Nd/Zn)−Zr alloys [J]. Materials Science and Engineering A, 2019, 762: 138080.

[7] XU C, ZHENG M Y, XU S W, WU K, WANG E D, KAMADO S, WANG G J, LV X Y. Ultra high-strength Mg−Gd−Y−Zn−Zr alloy sheets processed by large-strain hot rolling and ageing [J]. Materials Science and Engineering A, 2012, 547: 93−98.

[8] XU C, NAKATA T, QIAO X G, ZHENG M Y, WU K, KAMADO S. Ageing behavior of extruded Mg−8.2Gd−3.8Y−1.0Zn−0.4Zr(wt.%) alloy containing LPSO phase and γ′ precipitates [J]. Scientific Reports, 2017, 7: 43391.

[9] ZHOU X J, LIU C M, GAO Y H, JIANG S N, LIU W H, LU L W. Microstructure and mechanical properties of extruded Mg−Gd−Y−Zn−Zr alloys filled with intragranular LPSO phases [J]. Materials Characterization, 2018, 135: 76−83.

[10] CHEN D J, ZHANG K, LI T, LI X G, LI Y J, MA M L, SHI G L, YUAN J W. Weak strengthening effect of the precipitated lamellar phase in the homogenized Mg−8Gd−4Y−1.6Zn−0.5Zr (wt.%) alloy followed by furnace cooling [J]. Materials Science and Engineering A, 2019, 744: 1−9.

[11] NIE J F. Precipitation and hardening in magnesium alloys [J]. Metallurgical and Materials Transactions A, 2012, 43(11): 3891−3939.

[12] ZHENG J X, LI Z, TAN L D, XU X S, LUO R C, CHEN B. Precipitation in Mg−Gd−Y−Zr alloy: Atomic-scale insights into structures and transformations [J]. Materials Characterization, 2016, 117: 76−83.

[13] ZHANG Y, RONG W, WU Y J, PENG L M, NIE J F, BIRBILISC N. A detailed HAADF-STEM study of precipitate evolution in Mg−Gd alloy [J]. Journal of Alloys and Compounds, 2019, 777: 531−543.

[14] HE S M, ZENG X Q, PENG L M, GAO X, NIE J F, DING W J. Precipitation in a Mg−10Gd−3Y−0.4Zr (wt.%) alloy during isothermal ageing at 250 °C [J]. Journal of Alloys and Compounds, 2006, 421: 309−313.

[15] LI T, DU Z W, ZHANG K, LI X G, YUAN J W, LI Y J, MA M L, SHI G, FU X, HAN X L. Characterisation of precipitates in a Mg−7Gd−5Y−1Nd−0.5Zr alloy aged to peak-ageing plateau [J]. Journal of Alloys and Compounds, 2013, 574: 174−180.

[16] XUE Z Y, REN Y J, LUO W B, ZHENG R P, XU C. Effect of aging treatment on the precipitation behavior and mechanical properties of Mg−9Gd−3Y−1.5Zn−0.5Zr alloy [J]. Journal of Materials Engineering and Performance, 2017, 26(12): 5963−5972.

[17] HAGIHARA K, OKAMOTO T, IZUNO H, YAMASAKI M, MATSUSHITA M, NAKANO T, KAWAMURA Y. Plastic deformation behavior of 10H-type synchronized LPSO phase in a Mg−Zn−Y system [J]. Acta Materialia, 2016, 109: 90−102.

[18] ZHU Y M, MORTON A J, NIE J F. The 18R and 14H long-period stacking ordered structures in Mg−Y−Zn alloys [J]. Acta Materialia, 2010, 58: 2936−2947.

[19] ABE E, ONO A, ITOI T, YAMASAKI M, KAWAMURA Y. Polytypes of long-period stacking structures synchronized with chemical order in a dilute Mg−Zn−Y alloy [J]. Philosophical Magazine Letters, 2011, 91(10): 690−696.

[20] KIM J K, KO W S, SANDLOBES S, HEIDELMANN M, GRABOWSKI B, RAABE D. The role of metastable LPSO building block clusters in phase transformations of an Mg−Y−Zn alloy [J]. Acta Materialia, 2016, 112: 171−183.

[21] LI Y X, ZHU G Z, QIU D, YIN D D, RONG Y H, ZHANG M X. The intrinsic effect of long period stacking ordered phases on mechanical properties in Mg-RE based alloys [J]. Journal of Alloys and Compounds, 2016, 660: 252−257.

[22] LI Y X, YANG C L, ZENG X Q, JIN P P, QIU D, DING W J. Microstructure evolution and mechanical properties of magnesium alloys containing long period stacking ordered phase [J]. Materials Characterization, 2018, 141: 286−295.

[23] ZHENG J X, CHEN B. Interactions between long-period stacking ordered phase and β' precipitate in Mg−Gd−Y−Zn−Zr alloy: Atomic-scale insights from HAADF-STEM [J]. Materials Letters, 2016, 176: 223−227.
[24] LI M, WANG X, FENG Q Y, WANG J, XU Z, ZHANG P H. The effect of morphology of the long-period stacking ordered phase on mechanical properties of the Mg−7Gd−3Y−1Nd−1Zn−0.5Zr (wt.%) alloy [J]. Materials Characterization, 2017, 125: 123−133.
[25] LIU W, DU Z W, LI T, ZHANG K, HAN X L, PENG Y G, ZHANG J, YUAN J W, LIU S F, PANG Z. On the precipitate evolution in a Mg−7Gd−3Y−1Nd−1Zn−0.5Zr alloy during isothermal ageing at 240 °C [J]. Transactions of Nonferrous Metals Society of China, 2019, 29(10): 2047−2055.
[26] NIE J F, WILSON N C, ZHU Y M, XU Z. Solute clusters and GP zones in binary Mg-RE alloys [J]. Acta Materialia, 2016, 106: 260−271.
[27] XU Z, WEYLAND M, NIE J F. Shear transformation of coupled β_1/β' precipitates in Mg−RE alloys: A quantitative study by aberration corrected STEM [J]. Acta Materialia, 2014, 81: 58−70.
[28] WANG D, FU P H, PENG L M, WANG Y X, DING W J. Development of high strength sand cast Mg−Gd−Zn alloy by co-precipitation of the prismatic β' and β_1 phases [J]. Materials Characterization, 2019, 153: 157−168.
[29] ZHANG Y, ZHU Y M, RONG W, WU Y J, PENG L M, NIE J F, BIRBILIS. On the precipitation in an Ag-containing Mg−Gd−Zr alloy [J]. Metallurgical and Materials Transactions A, 2018, 49(2): 673−694.
[30] LIU H, XU W F, WILSON N C, PENG L M, NIE J F. Formation of and interaction between β'_F and β' phases in a Mg−Gd alloy [J]. Journal of Alloys and Compounds, 2017, 712: 334−344.
[31] LIU H, ZHU Y M, WILSON N C, NIE J F. On the structure and role of β'_F in β_1 precipitation in Mg−Nd alloys [J]. Acta Materialia, 2017, 133: 408−426.
[32] HONMA T, OHKUBO T, KAMADO S, HONO K. Effect of Zn additions on the age-hardening of Mg−2.0Gd−1.2Y−0.2Zr alloys [J]. Acta Materialia, 2007, 55: 4137−4150.

含 14H-LPSO 结构的 Mg−7Gd−3Y−1Nd−1Zn−0.5Zr 合金在 240 °C 时效过程中析出相的演化

彭永刚[1,2,3,4]，杜志伟[1,2,3,4]，刘 伟[5]，李永军[6]，李 婷[1,2,3,4]，
韩小磊[1,2]，马鸣龙[6]，庞 铮[1,2,3,4]，袁家伟[6]，石国梁[6]

1. 有研科技集团有限公司 国家有色金属及电子材料分析测试中心，北京 100088；
2. 国标（北京）检验认证有限公司，北京 100088；
3. 北京有色金属研究总院，北京 100088；
4. 国合通用测试评价认证股份公司，北京 100088；
5. 北京市春立正达医疗器械股份有限公司，北京 101100；
6. 有研工程技术研究院有限公司 有色金属材料制备加工国家重点实验室，北京 101407

摘 要：通过 TEM 与 HAADF-STEM 技术分析含 14H-LPSO 结构的 Mg−7Gd−3Y−1Nd−1Zn−0.5Zr (质量分数，%) 合金在 240 °C 时效过程中析出相的形貌和晶体学特征。薄片状 14H-LPSO 结构在 500 °C、2 h 热处理过程中析出，而 β 型析出相在 240 °C 时效过程中析出。14H-LPSO 结构沿 $[0001]_\alpha$ 方向的原子堆垛顺序为 ABABCACACACBABA。240 °C 时效 2 h 时，β 型析出相为有序固溶团簇、之字形 GP 区和少量的 β'相。240 °C 时效 18 h 达到峰值，相应的布氏硬度值为 112，β 型析出相为 β'相和局部富 RE 结构。240 °C 时效 100 h 时，β 型析出相为 β'、β_1 和 β'_F。β'相不经过 β''相直接从之字形 GP 区形核，然后通过 $\beta'\rightarrow\beta'_F\rightarrow\beta_1$ 转变成 β_1 相。Zn 的添加不仅可以形成 LPSO 结构，而且参与 β_1 相的形成。LPSO 结构阻碍 β'和 β_1 相沿$\langle 0001\rangle_\alpha$的生长。

关键词：镁合金；时效；析出相；长程堆垛有序 (LPSO) 结构；HAADF-STEM

(Edited by Bing YANG)